Structure Determination of the Ferroelastic Triple-Twinned Phase of $K_3Na(SeO_4)_2$ at 291 K and its Parent Phase at 390 K

By J. Fábry* and T. Breczewski†

Departamento de Física de la Materia Condensada, Facultad de Ciencias, Universidad del Pais Vasco, Apdo. 644, 48080 Bilbao, Spain

and V. Petříček

Institute of Physics, Czechoslovak Academy of Sciences, Cukrovarnicka 10, 162 00 Praha 6, Czechoslovakia

Abstract

$K_3Na(SeO_4)_2$, $M_r = 426.19$, $\lambda(Mo\ K\alpha) = 0.71073$ Å, two phases. At 291 K, monoclinic, $C2/c$, $a = 10.162$ (2), $b = 5.867$ (1), $c = 15.021$ (2) Å, $\beta = 90.00$ (1)°, $V = 895.56$ Å^3, $\mu = 96.29$ cm^{-1}, $Z = 4$, $F(000) = 800$, $D_x = 3.160$ g cm^{-3}, $R = 0.0202$ for 1779 observed reflections. Lattice parameters of the pseudohexagonal cell: $a = 5.867$ (1), $b = 5.867$ (1), $c = 15.021$ (2) Å, $\alpha = 90.0$, $\beta = 90.00$ (1), $\gamma = 120.0°$. At 390 K, trigonal, $P\bar{3}m1$, $a = 5.906$ (3), $c = 7.552$ (1) Å, $V = 228.13$ Å^3, $\mu = 94.50$ cm^{-1}, $Z = 1$, $F(000) = 200$, $D_x = 3.101$ g cm^{-3}, $R = 0.0126$ for 222 observed reflections. The high-temperature phase is isomorphous with the room-temperature structures of $K_3Na(CrO_4)_2$ and $K_3Na(SO_4)_2$ and at 346 K undergoes a reversible ferroelastic phase transition from point group $\bar{3}m1$ to $2/m$. Below this transition point the c axis, originally coincident with the trigonal axis, doubles its length. As a consequence, below the transition point the crystals are triple-twinned with a 120° domain structure, and the mirror plane is replaced by the glide plane c. Both structures consist of $[SeO_4]^{2-}$ tetrahedral anions, Na cations coordinated by six O atoms in a deformed octahedron, and two crystallographically independent K(1) and K(2) cations with 10 and 12 O-atom coordination, respectively. The phase transition is accompanied by the shift of K(1) and K(2) cations as well as by the shift and tilting of $[SeO_4]^{2-}$ by 7.6 (1)°. The phase transition mainly affects the environment of K(2). The cation–O-atom distances and temperature factor as well as the bond-valence sums indicate that this K atom is the most loosely bound atom in the high- and low-temperature phases. The thermal stability of isomorphous $K_3Na(CrO_4)_2$ and

$K_3Na(SO_4)_2$ is related to the bonding of this cation.

Introduction

The aim of the present work was to determine the structures of $K_3Na(SeO_4)_2$ below and above the transition point and to compare them with the already determined (room temperature) isostructural trigonal phases of $K_3Na(SO_4)_2$ (Okada & Ossaka, 1980) and $K_3Na(CrO_4)_2$ (Madariaga & Breczewski, 1990) which belong to the glaserite family. Powder diffraction patterns have also been reported for the related compounds $K_3Na(MoO_4)_2$ (PDF 28-801), $K_3Na(WO_4)_2$ (PDF 28-802) and $Rb_{2.7}Na_{1.3}(CrO_4)_2$ (PDF 38-1185). (The numbers given in parentheses refer to the Powder Diffraction File.)

In addition to these compounds with oxygen-containing anions (Bergerhoff, Hundt, Sievers & Brown, 1983), $Rb_3Na(BeF_4)_2$, $K_3Na(BeF_4)_2$, $Tl_3Na(BeF_4)_2$ and $(NH_4)_3Na(BeF_4)_2$ are also isostructural with $K_3Na(SO_4)_2$ (Pontonnier, Caillet & Aleonard, 1972).

Finally, Tl_2WO_4 at room temperature (Okada, Ossaka & Iwai, 1979) and presumably Tl_2MoO_4 (Gaultier & Pannetier, 1972) between 311 and 673 K also belong to the glaserite family.

$K_3Na(SeO_4)_2$ exhibits two phase transitions at $T = 334$ and 346 K (Krajewski, Piskunowicz & Mroz, 1993). The latter is accompanied by anomalies in DTA curves, thermal expansion and dielectric constants. The phase transition at 334 K was deduced from the temperature dependence of the elastic constants C_{ij} (this phenomenon is related to the acoustic phonon softening). Furthermore, it was determined from the studies of Brillouin shifts (Mroz, Kiefte, Clouter & Tuszynski, 1992) that the elastic constant C_{33} exhibits anomalous behaviour at $T = 346$ K, and C_{44} has two minima at 334 and 346 K. The rest of the elastic constants exhibit anomalies at $T = 334$ K.

The ferroelastic domains which are reorientable under external force are clearly observable below

---

* On leave of absence from the Institute of Physics of the Czechoslovak Academy of Sciences, Na Slovance 2, 180 40 Praha 8, Czechoslovakia.

† On leave of absence from the Institute of Physics, A. Mickiewicz University, Grunwaldzka 6, 60-780 Poznań, Poland.

334 K. Neither piezo- nor pyroelectric effects were detected (Krajewski, Piskunowicz & Mroz, 1993).

$K_3Na(CrO_4)_2$ has been reported to undergo a ferroelastic phase transition at 239 K (Krajewski, Mroz, Piskunowicz & Breczewski, 1990) while in $K_3Na(SO_4)_2$ no phase transition was found in the region 100–300 K (Krajewski, 1990). The ferroelastic phase transition of $K_3Na(CrO_4)_2$ is reported to be of an order–disorder type and neither pyroelectric nor piezoelectric phenomena were observed in the ferroelastic phase of this crystal. All experimental data suggest that $K_3Na(CrO_4)_2$ undergoes a ferroelastic phase transition accompanied by change of the crystal class: $\bar{3}m1 \rightarrow 2/m$. It was supposed that $K_3Na(SeO_4)_2$ might have been isostructural with $K_3Na(CrO_4)_2$ also in the low-temperature phase. However, until now no structure determination nor crystal data of any ferroelastic phase regarding these compounds has been reported.

Experimental

Colourless crystals of the title compound were grown from an aqueous stoichiometric solution of K_2SeO_4 and Na_2SeO_4. From our optical observations it followed that the samples were biaxial up to 346 K and the ferroelastic domains gradually faded above 334 K with increasing temperature. When passing 334 K during heating the domains became dimmed.

A set of precession photographs taken at 290, 338 and 352 K revealed doubling of the c axis below 346 K and systematic extinctions for $00l$; $l = 2n + 1$. The newly developed reflections which caused doubling of the c axis were observed in the plane $h - h0l$ (pseudohexagonal unit cell considered) both at 338 and 290 K. It is worthwhile noting that the intensities of the newly developed reflections diminish with increasing temperature and that these reflections could only have been detected on overexposed photographs.

From the absence of piezo- and pyroelectric effects it follows that the low-temperature phase (LTP) was expected to be centrosymmetric. The high-temperature phase (HTP) was supposed to be isomorphous with the room-temperature phases of $K_3Na(CrO_4)_2$ and $K_3Na(SO_4)_2$ with the space group $P\bar{3}m1$.

Taking into account the orientation of the vanished trigonal axis with respect to the symmetry elements of the supposed crystal class $2/m$ then the observed extinctions were expected to be caused by the glide plane c. The rest of the extinctions (h, 0, l; $h \neq 0$, $l = 2n + 1$) could not be observed because of overlapping of reflections from two other domains.

A crystal with well developed faces of the approximate size $0.15 \times 0.16 \times 0.30$ mm was mounted on an Enraf–Nonius CAD-4 diffractometer. Graphite-

Table 1. *Data-collection and refinement parameters for* $K_3Na(SeO_4)_2$

	Low-temperature phase	High-temperature phase
Temperature (K)	291 (1)	390 (8)
Scan type	ω–2θ	ω 2θ
ω-scan width ($^\circ$)	1.50 + 0.35tanθ	1.90 + 0.35tanθ
Horizontal aperture (mm)	1.50 + 2.20tanθ	1.50 + 2.20tanθ
Vertical aperture (mm)	4	4
Min./max. scan speed ($^\circ$ min^{-1})	1.498, 5.493	1.177, 5.493
Maximal final scan time (s)	120	120
Measured region θ ($^\circ$)	≤ 28	≤ 28
h,k,l range	$\langle -13,13\rangle, \langle -7,7\rangle, \langle 0,19\rangle$ U U $\langle -13,13\rangle, \langle 0,7\rangle, \langle -19,1\rangle$	$\langle -7,7\rangle, \langle -7,7\rangle, \langle 0,9\rangle$ U U $\langle -7,7\rangle, \langle 0,7\rangle, \langle -9,1\rangle$
No. of measured reflections	3415	1745
No. of observed reflections [$I \geq 3\sigma(I)$]	2824	1699
Averaging No. of all/obs. reflections		
used in refinement	2182/1779	240/222
used in Fourier synthesis	1195/970	240/222
Estimated R factors, all/obs. reflections	0.024/0.015	0.018/0.016
R_{int}	0.011	0.028
Min./max. transmission factors for reflections	0.2455/0.4527 $(372)/(\bar{1},\bar{1},19)$	0.2533/0.4552 $(\bar{5}21)/(119)$
Extinction correction/isotropic Lorentzian distribution (g)	0.246 (9) × 10^{-4}	0.44 (2) × 10^{-4}
Domain fractions determined from overlapped space-group extinct reflections/by refinement		
f_1	0.478 (25)/0.473 (4)	
f_2	0.329 (42)/0.328 (3)	
f_3	0.193 (41)/0.199 (3)	
No. of refined parameters	69	21
Weighting scheme, w^{-1} =	$\sigma^2(F_o) + (0.01 F_o)^2$	$\sigma^2(F_o) + (0.01 F_o)^2$
R for all reflections	0.0275	0.0140
wR for all reflections	0.0279	0.0196
R for observed reflections only	0.0202	0.0126
wR for observed reflections only	0.0266	0.0192
S	1.393	1.034
$\Delta\rho_{max}$ (e Å^{-3})	2.395	0.259
$\Delta\rho_{min}$ (e Å^{-3})	−1.657	−0.480
$(\Delta/\sigma)_{max}$	≤0.03	≤0.01

monochromated Mo $K\alpha$ radiation was used. Unit-cell parameters were refined from 25 reflections ($4 < \theta < 16$ and $7 < \theta < 25°$ for the low- and high-temperature phases, respectively).

The lattice parameters determined from the triple-twinned monocrystal reflections are biased by systematical error since these reflections are super-imposed diffractions from each domain the lattices of which need not necessarily overlap exactly. Thus the single-crystal diffractometer will tend to centre a reflection along the centroid of the bundle of super-imposed diffractions. In order to check the lattice parameters which were obtained from the single-crystal diffractometer experiment a powder diffraction experiment was performed on a Stoe focusing monochromatic transmission diffractometer equipped with a linear position detector. The powdered sample was inserted into a Lindemann capillary of diameter 0.3 mm. The measured region was 5.00–84.89° (2θ); λ(Cu $K\alpha_1$) = 1.54056 Å. Figure of merit $F(N_{obs}/\Delta_{average})$: $F(45/0.007) = 15.0$ for 2θ error window = 0.047 and the refined lattice parameters are: $a = 10.159$ (2), $b = 5.863$ (3), $c = 15.018$ (2) Å, $\beta = 89.994$ (12)°. For 2θ error window = 0.045 [$F(45/0.006) = 18.9$] the refined lattice

Table 2. *Relevant transformations and relations used in the structure determination of the low-temperature phase of* $K_3Na(SeO_4)_2$

(1) Expression for transformation of indices from the primitive pseudohexagonal unit cell to the standard monoclinic C-centred (pseudoorthorhombic) unit cell

$$\begin{bmatrix} h \\ k \\ l \end{bmatrix}^a = \begin{bmatrix} -1 & 1 & 0 \\ -1 & -1 & 0 \\ 0 & 0 & 1 \end{bmatrix} \begin{bmatrix} h \\ k \\ l \end{bmatrix}^h$$

(2) Relations for superposition of indices from pertinent domains expressed in the pseudohexagonal and pseudoorthorhombic unit cells

$$\begin{bmatrix} h \\ k \\ l \end{bmatrix}^{h1} = \begin{bmatrix} 0 & 1 & 0 \\ -1 & -1 & 0 \\ 0 & 0 & 1 \end{bmatrix} \begin{bmatrix} h \\ k \\ l \end{bmatrix}^h \quad \begin{bmatrix} h \\ k \\ l \end{bmatrix}^{h2} = \begin{bmatrix} -1 & -1 & 0 \\ 1 & 0 & 0 \\ 0 & 0 & 1 \end{bmatrix} \begin{bmatrix} h \\ k \\ l \end{bmatrix}^h$$

$$\begin{bmatrix} h \\ k \\ l \end{bmatrix}^{o1} = \begin{bmatrix} -\frac{1}{2} & \frac{3}{2} & 0 \\ -\frac{1}{2} & -\frac{1}{2} & 0 \\ 0 & 0 & 1 \end{bmatrix} \begin{bmatrix} h \\ k \\ l \end{bmatrix}^o \quad \begin{bmatrix} h \\ k \\ l \end{bmatrix}^{o2} = \begin{bmatrix} -\frac{1}{2} & -\frac{3}{2} & 0 \\ \frac{1}{2} & -\frac{1}{2} & 0 \\ 0 & 0 & 1 \end{bmatrix} \begin{bmatrix} h \\ k \\ l \end{bmatrix}^o$$

(3) Expression for the ferroelastic transformations of coordinates in the pseudohexagonal unit cell (see also Table 3)

$$\begin{bmatrix} x \\ y \\ z \end{bmatrix}^A = \begin{bmatrix} -1 & 0 & 0 \\ 1 & -1 & 0 \\ 0 & 0 & 1 \end{bmatrix} \begin{bmatrix} x \\ y \\ z \end{bmatrix} \quad \begin{bmatrix} x \\ y \\ z \end{bmatrix}^B = \begin{bmatrix} -1 & 1 & 0 \\ -1 & 0 & 0 \\ 0 & 0 & 1 \end{bmatrix} \begin{bmatrix} x \\ y \\ z \end{bmatrix}$$

(4) Twofold axis operators of the non-standard space group $\overline{P}2''_c$ and the other two space groups the symmetry operators of which are rotated by 120 and 240° in an anticlockwise direction with respect to those in $\overline{P}2''_c$. The remaining group operators are obtained by multiplication of these operators with inversion and identity operators. These non-standard space groups are isomorphous with the $C2/c$ space group

$$\overline{P}2''_c \qquad\qquad \overline{P}2''_c (120°) \qquad\qquad \overline{P}2''_c (240°)$$

$$\begin{bmatrix} 0 & 1 & 0 \\ 1 & 0 & 0 \\ 0 & 0 & -1 \end{bmatrix} \begin{bmatrix} 0 \\ 0 \\ \frac{1}{2} \end{bmatrix} \quad \begin{bmatrix} 1 & -1 & 0 \\ 0 & -1 & 0 \\ 0 & 0 & -1 \end{bmatrix} \begin{bmatrix} 0 \\ 0 \\ \frac{1}{2} \end{bmatrix} \quad \begin{bmatrix} -1 & 0 & 0 \\ -1 & 1 & 0 \\ 0 & 0 & -1 \end{bmatrix} \begin{bmatrix} 0 \\ 0 \\ \frac{1}{2} \end{bmatrix}$$

parameters are $a = 10.163$ (3), $b = 5.857$ (5), $c = 15.019$ (2) Å, $\beta = 90.016$ (18)°. From these data it is obvious that the deformation of the lattice from a hexagonal metric is very small and beyond the precision of either powder or single-crystal experiments.

The elevated temperature was provided by a stream of heated air. ω/θ plots indicated that reflection profiles were not significantly affected by the phase transition and that an $\omega/2\theta$ scan was the most appropriate for data collection below as well as above the phase transition. Monitoring reflections for the LTP ($31\bar{4}$, $\bar{1}16$, $11\bar{6}$, $\bar{2}42$, 201) and the HTP ($\bar{2}12$, $01\bar{3}$, $10\bar{3}$, 311, $\bar{1}10$) were recorded every 3600 s and their intensity oscillations did not exceed 3 and 7% from their average values for the LTP and HTP, respectively.

Absorption (Gaussian integration) and intensity corrections for the variance of intensities of standard reflections were provided by the program system *XRAY*72 (Stewart, Kruger, Ammon, Dickinson &

Table 3. *Atomic positional parameters for the low-temperature phase expressed in the pseudohexagonal primitive unit cell with e.s.d.'s in parentheses*

The first line refers to the non-standard space group $\overline{P}2''_c$; the second and the third lines to the space groups which are obtained by rotation of the symmetry elements in $\overline{P}2''_c$ by 120 and 240° about the c axis in an anticlockwise direction, respectively.

	x	y	z
Se	0.34192 (6)	0.67316 (6)	0.13675 (1)
Se^A	0.32676 (6)	0.66867 (10)	0.13675 (1)
Se^B	0.33133 (1)	0.65809 (6)	0.13675 (1)
K(1)	0.3430 (2)	0.6792 (2)	0.41292 (3)
K(1)^A	0.3208 (2)	0.6638 (3)	0.41292 (3)
K(1)^B	0.3362 (3)	0.6570 (2)	0.41292 (3)
K(2)	0.0267 (1)	0.0267 (1)	$\frac{1}{4}$
K(2)^A	0.9732 (1)	0	$\frac{1}{4}$
K(2)^B	0	0.9732 (1)	$\frac{1}{4}$
Na	0	0	0
Na^A	0	0	0
Na^B	0	0	0
O(1)	0.3016 (7)	0.6435 (8)	0.2434 (1)
O(1)^A	0.3566 (8)	0.6582 (14)	0.2434 (1)
O(1)^B	0.3418 (14)	0.6984 (7)	0.2434 (1)
O(2)	0.2024 (7)	0.3829 (4)	0.0894 (2)
O(2)^A	0.6171 (4)	0.8195 (7)	0.0894 (2)
O(2)^B	0.1805 (7)	0.7977 (7)	0.0894 (2)
O(3)	0.6524 (3)	0.8316 (7)	0.1086 (2)
O(3)^A	0.1685 (7)	0.8208 (6)	0.1086 (2)
O(3)^B	0.1791 (6)	0.3476 (4)	0.1086 (2)
O(4)	0.2030 (6)	0.8332 (6)	0.0966 (4)
O(4)^A	0.1668 (6)	0.3697 (8)	0.0966 (4)
O(4)^B	0.6302 (8)	0.7970 (6)	0.0966 (4)

Hall, 1972); Lp correction and calculation of structure factors and their e.s.d.'s as well as their averaging was carried out by the conversion program to the *SDS* system (Petříček & Malý, 1988). Square roots of intensities of the LTP were averaged with respect to the centre of symmetry. For the calculation of the Fourier synthesis of the LTP, however, a set of symmetry-independent reflections was selected. The *SDS* program was used for the rest of calculations except the bond-length correction for the temperature movement which was carried out by the program *PARST* (Nardelli, 1983). Scattering factors including anomalous-dispersion corrections were taken from Cromer & Mann (1968) and *International Tables for X-ray Crystallography* (1974, Vol. IV).

The structure of the HTP phase was determined by the solution of a Patterson synthesis. The starting model for the refinement of the LTP was calculated from the HTP. The geometry of the $[SeO_4]^{2-}$ anion and the values of the domain fractions, which were determined from the reflections superimposed on group-extinct reflections (see below), were kept fixed at the beginning of the refinement. The positions of O atoms were refined individually only after the isotropic refinement had converged. Unrestrained refinement of the $[SeO_4]^{2-}$ anion converged to a false minimum from the very beginning with a very distorted $[SeO_4]^{2-}$ anion. The refinement, assuming extinction of type I with isotropic Lorentzian distribution (Becker & Coppens, 1974), considerably lowered the R factor in both cases, from 0.0376 to 0.0126 for the HTP and from 0.0277 to 0.0202 for the LTP.

Refinement of the model of the LTP where K(2) occupied a centre of symmetry and the rest of atoms were shifted by $\langle 0,0,\frac{1}{4}\rangle$ resulted in a much higher R factor. The refinement in the $P\bar{1}$ space group with six domains (60° domain pattern) did not converge.

The difference Fourier synthesis* $\Delta\rho = V^{-1}\sum_h\Delta F(\mathbf{h})\exp(-2\pi\mathbf{hr})$, where $\Delta F(\mathbf{h}) = |F_o|/Sc - |F_c(\mathbf{h})|$ for a single domain crystal (Sc is a general scaling factor), is modified for a triple-twinned crystal (f_i are domain fraction parameters):

$$\Delta F(\mathbf{h}) = \{[(|F_o|^2/Sc^2) - f_2|F_c|_2^2 - f_3|F_c|_3^2]/f_1\}^{1/2} - |F_c|_1.$$

The refinement was also carried out in three non-conventional space groups in the pseudohexagonal primitive unit cell (Table 3). One of these space groups may be expressed as $\bar{P}2_c''$ (Hall, 1981) and the other two are obtained by rotation of symmetry

* Lists of structure factors and anisotropic thermal parameters have been deposited with the British Library Document Supply Centre as Supplementary Publication No. SUP 71062 (33 pp.). Copies may be obtained through The Technical Editor, International Union of Crystallography, 5 Abbey Square, Chester CH1 2HU, England. [CIF reference: AL0550]

Fig. 1. High-temperature phase of $K_3Na(SeO_4)_2$. Two unit cells which are linked by translation along the c axis are depicted.
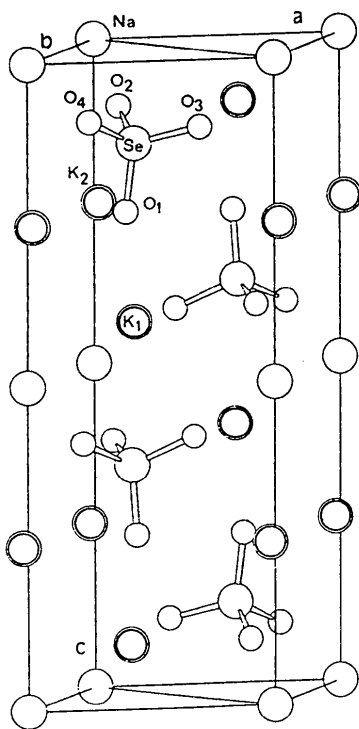
Fig. 2. Low-temperature phase of $K_3Na(SeO_4)_2$. Pseudohexagonal unit cell is depicted (space group $\bar{P}2_c''$).
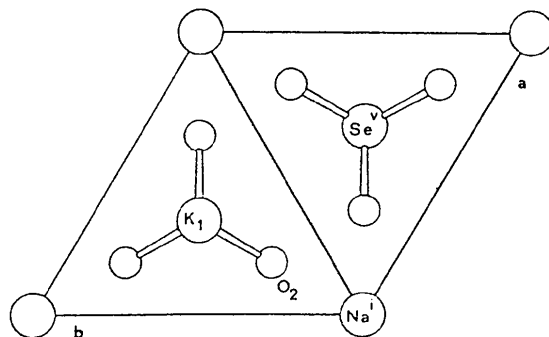
Fig. 3. View of the high-temperature phase of $K_3Na(SeO_4)_2$ along the c axis (symmetry codes are given in Table 6).
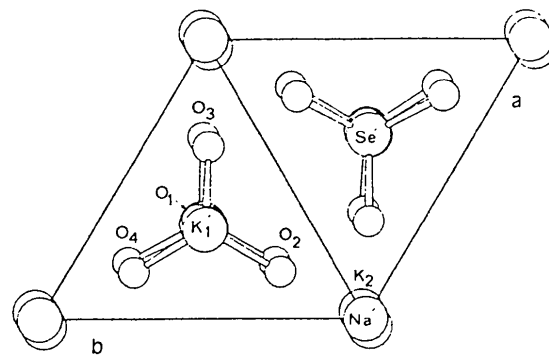
Fig. 4. View of the low-temperature phase of $K_3Na(SeO_4)_2$ along the c axis of the pseudohexagonal unit cell (space group $\bar{P}2_c''$). Se', K(1)' and Na' are connected with the atomic positions given in Table 3 by the symmetry transformations $(1 - x, 1 - y, 1 - z)$, $(1 - y, 1 - x, \frac{1}{2} + z)$ and $(x, y, 1 + z)$, respectively.

Table 4. *Atomic positional parameters and anisotropic thermal parameters* U_{ij} (Å²) *of the high-temperature phase of* K₃Na(SeO₄)₂ (391 K) *with e.s.d.'s in parentheses*

The anisotropic temperature factors are of the form: $U_{ij} = \exp[-2\pi^2(U_{11}h^2a^{*2} + U_{22}k^2b^{*2} + U_{33}l^2c^{*2} + 2U_{12}hka^*b^* + 2U_{13}hla^*c^* + 2U_{23}klb^*c^*)]$.

	x	y	z	U_{11}	U_{22}	U_{33}	U_{12}	U_{13}	U_{23}
Se	⅓	⅔	0.27241 (4)	0.0184 (2)	0.0184 (2)	0.0173 (2)	0.0092 (1)	0	0
K(1)	⅓	⅔	0.8240 (1)	0.0303 (3)	0.0303 (3)	0.0277 (5)	0.0151 (2)	0	0
K(2)	0	0	½	0.0519 (6)	0.0519 (6)	0.0285 (7)	0.0259 (3)	0	0
Na	0	0	0	0.0245 (7)	0.0245 (7)	0.0307 (11)	0.0122 (3)	0	0
O(1)	⅓	⅔	0.4852 (5)	0.0918 (22)	0.0918 (22)	0.0207 (16)	0.0459 (11)	0	0
O(2)	0.1842 (2)	0.3685 (4)	0.1965 (3)	0.0391 (8)	0.0241 (9)	0.0649 (11)	0.0121 (4)	-0.0086 (5)	-0.0172 (9)

Table 5. *Atomic positional parameters and anisotropic thermal parameters* U_{ij} (Å²) *of the low-temperature phase of* K₃Na(SeO₄)₂ (291 K) *with e.s.d.'s in parentheses*

The anisotropic temperature factors are of the form: $U_{ij} = \exp[-2\pi^2(U_{11}h^2a^{*2} + U_{22}k^2b^{*2} + U_{33}l^2c^{*2} + 2U_{12}hka^*b^* + 2U_{13}hla^*c^* + 2U_{23}klb^*c^*)]$.

	x	y	z	U_{11}	U_{22}	U_{33}	U_{12}	U_{13}	U_{23}
Se	0.16566 (5)	0.49242 (3)	0.13675 (1)	0.0143 (3)	0.0089 (2)	0.0096 (1)	-0.00004 (7)	0.0008 (2)	0.00013 (5)
K(1)	0.1681 (1)	0.48888 (7)	0.41293 (3)	0.0212 (6)	0.0177 (5)	0.0159 (2)	-0.0005 (2)	-0.0009 (5)	0.0015 (1)
K(2)	0	0.9733 (1)	¼	0.0374 (9)	0.0278 (6)	0.0171 (3)	0	0.0022 (7)	0
Na	0	0	0	0.0181 (16)	0.0137 (14)	0.0175 (5)	0.0001 (4)	0.0013 (16)	0.0010 (3)
O(1)	0.1709 (7)	0.5275 (3)	0.2434 (1)	0.0585 (28)	0.0477 (19)	0.0106 (8)	-0.0020 (14)	-0.0025 (19)	-0.0071 (7)
O(2)	0.0903 (3)	0.7074 (5)	0.0894 (2)	0.0259 (22)	0.0202 (15)	0.0331 (12)	0.0064 (11)	-0.0041 (16)	0.0083 (11)
O(3)	0.0896 (3)	0.2580 (5)	0.1086 (2)	0.0239 (22)	0.0167 (15)	0.0383 (13)	-0.0039 (11)	-0.0073 (16)	-0.0050 (11)
O(4)	0.3151 (4)	0.4819 (5)	0.0966 (4)	0.0160 (15)	0.0311 (19)	0.0434 (22)	0.0017 (13)	0.0144 (15)	0.0043 (15)

elements within the unit cell by 120 and 240° about the *c* axis (Table 2). Refinement in these non-standard space groups yields the coordinates of atoms in the pseudohexagonal unit cell which are mutually related by the pseudotrigonal rotation axis. This axis coincides with the *c* axis and the differences in coordinates between the atoms which are related by this pseudotrigonal rotation axis determine atomic displacement vectors **Δ** (Abrahams & Keve, 1971). The values of **Δ** are given in Table 7. The other relevant information about the experiment and refinement of both structures is given in Table 1.

Discussion

The structures of the HTP and the LTP are shown in Figs. 1–4, and their coordinates with temperature factors U_{ij} are given in Tables 4 and 5, respectively. Table 6 contains relevant interatomic distances and angles of both structures.

The structure determination proved that the HTP is isostructural with K₃Na(CrO₄)₂ and K₃Na(SO₄)₂ room-temperature phases.

The diffraction pattern of the LTP offers a possibility to confirm the correctness of the choice of the space group and to evaluate values of the domain fractions independently of the refinement of the structure.

Let us suppose the space group *C2/c* and let us consider an extinct reflection $(h0l)_1$; $h = 2n$, $l = 2n + 1$ of the first domain. Two other reflections are superimposed on this reflection: $(-h/2, -h/2, l)_2$ and $(-h/2, h/2, l)_3$ of the second and the third domain. [The twinning operations (see Table 2) are $(-\frac{1}{2},\frac{3}{2},0|-\frac{1}{2},-\frac{1}{2},0|0,0,1)$ and $(-\frac{1}{2},-\frac{3}{2},0|\frac{1}{2},-\frac{1}{2},0|0,0,1)$, respectively.] Each measured intensity $I^o(h0l)$,

$I^o(-h/2,h/2,l)$ and $I^o(-h/2,-h/2,l)$; $h = 2n$, $l = 2n + 1$ may be then expressed as follows:

$$I''(h0l) \quad = \quad V_2I(-h/2,-h/2,l)+V_3I(-h/2,h/2,l)$$

$$I''(-h/2,h/2,l) \quad = V_1I(-h/2,h/2,l) + \quad\quad V_3I(-h/2,-h/2,l)$$

$$I''(-h/2,-h/2,l) = V_1I(-h/2,-h/2,l) + V_2I(-h/2,h/2,l).$$

Each column on the right-hand side of the equations applies for each particular domain while V_i; $i = 1, 3$ means its volume and $I(h,k,l)$ is intensity scattered by the unit volume. Since $I(-h/2,h/2,l)$ and $I(-h/2,-h/2,l)$; $h = 2n$, $l = 2n + 1$ are space-group equivalents the domain fractions f_i may be determined straightforwardly from the equations given above because they are proportional to V_i.

The measured data contained 19 reflection triplets of this type which fulfilled the condition that the average $I/\sigma(I)$ within each triplet is > 10. The unweighted mean values of the domain fractions determined from the equations given above fit well with the values determined by the structure refinement (Table 1).

The $[SeO_4]^{2-}$ molecule is little distorted from the ideal tetrahedral configuration both in the HTP and the LTP. The shorter Se—O(1) distances indicate librational movement at both temperatures. Somewhat longer Se—O bond distances in the LTP than in the HTP are in accordance with assumption of more intensive librational movement of $[SeO_4]^{2-}$ at elevated temperatures. The Se—O bond-length correction – 'riding motion' which was based on the ideas of Busing & Levy (1964) – resulted in a more even distribution of Se—O distances.

The bond distances between cations and O atoms are shorter on the whole in the LTP than in the HTP. In order to compare contributions of O atoms

Table 6. *Selected interatomic distances (Å) and angles (°) of the low- and high-temperature phases with e.s.d.'s in parentheses*

	291 K		390 K
Coordination of K(1)			
K(1)—O(1)	2.557 (2)	K(1)—O(1)	2.558 (4)
K(1)—O(2')	2.922 (4)	K(1)—O(2')	2.963 (2)
K(1)—O(2")	2.959 (4)	K(1)—O(2")	2.963 (2)
K(1)—O(3")	2.943 (4)	K(1)—O(2")	2.963 (2)
K(1)—O(3')	2.966 (3)	K(1)—O(2")	2.963 (2)
K(1)—O(4")	2.901 (3)	K(1)—O(2"')	2.963 (2)
K(1)—O(4")	2.983 (3)	K(1)—O(2")	2.963 (2)
∅	2.945		2.963
K(1)—O(2"')	2.996 (3)	K(1)—O(2")	3.200 (2)
K(1)—O(4"')	3.143 (5)	K(1)—O(2"')	3.200 (2)
K(1)—O(3"')	3.388 (3)	K(1)—O(2')	3.200 (2)
∅	3.175		3.200
Coordination of K(2)			
K(2)—O(2')	3.016 (3)	K(2)—O(2)	2.967 (2)
K(2)—O(2"')	3.016 (3)	K(2)—O(2')	2.967 (2)
K(2)—O(3)	2.851 (3)	K(2)—O(2")	2.967 (2)
K(2)—O(3')	2.851 (3)	K(2)—O(2")	2.967 (2)
K(2)—O(4")	2.973 (5)	K(2)—O(2"')	2.967 (2)
K(2)—O(4")	2.973 (5)	K(2)—O(2"')	2.967 (2)
∅	2.947		2.967
K(2)—O(1)	3.688 (4)	K(2)—O(1ˣˈ')	3.4117 (1)
K(2)—O(1")	3.361 (7)	K(2)—O(1"')	3.4117 (1)
K(2)—O(1ˣ)	3.141 (4)	K(2)—O(1)	3.4117 (1)
K(2)—O(1')	3.688 (4)	K(2)—O(1ˣ')	3.4117 (1)
K(2)—O(1")	3.361 (7)	K(2)—O(1ˣ)	3.4117 (1)
K(2)—O(1"')	3.141 (4)	K(2)—O(1ˣ)	3.4117 (1)
∅	3.397		3.4117
Coordination of Na			
Na—O(2')	2.365 (3)	Na—O(2)	2.399 (2)
Na—O(2"')	2.365 (3)	Na—O(2"')	2.399 (2)
Na—O(3")	2.404 (3)	Na—O(2')	2.399 (2)
Na—O(3)	2.404 (3)	Na—O(2")	2.399 (2)
Na—O(4"')	2.377 (5)	Na—O(2"')	2.399 (2)
Na—O(4')	2.377 (5)	Na—O(2"")	2.399 (2)
∅	2.382		2.399
Coordination of Se			
Se—O(1)	1.616 (2) (1.642)*	Se—O(1)	1.607 (4) (1.653)*
Se—O(2)	1.638 (3) (1.648)*	Se—O(2)	1.629 (2) (1.654)*
Se—O(3)	1.634 (3) (1.647)*	Se—O(2"')	1.629 (2) (1.654)*
Se—O(4)	1.635 (4) (1.651)*	Se—O(2"')	1.629 (2) (1.654)*
O(1)—Se—O(2)	110.4 (2)	O(1)—Se—O(2)	110.59 (8)
O(1)—Se—O(3)	112.3 (2)	O(1)—Se—O(2"')	110.59 (8)
O(1)—Se—O(4)	109.9 (3)	O(1)—Se—O(2"')	110.59 (8)
O(2)—Se—O(3)	108.3 (2)	O(2)—Se—O(2"')	108.33 (7)
O(2)—Se—O(4)	107.7 (2)	O(2)—Se—O(2"')	108.33 (7)
O(3)—Se—O(4)	108.2 (2)	O(2"')—Se—O(2"")	108.33 (7)

Symmetry codes for the low-temperature phase: (i) $-x, y, -z + \frac{1}{2}$; (ii) $-x + \frac{1}{2}, y - \frac{1}{2}, -z + \frac{1}{2}$; (iii) $x, -y + 1, z + \frac{1}{2}$; (iv) $-x + \frac{1}{2}, y + \frac{1}{2}, -z + \frac{1}{2}$; (v) $x, y - 1, z$; (vi) $x - \frac{1}{2}, y - \frac{1}{2}, z$; (vii) $-x, y - 1, -z + \frac{1}{2}$; (viii) $-x, -y + 1, -z$; (ix) $-x, -y, -z$; (x) $-x + \frac{1}{2}, -y + \frac{1}{2}, -z$. Symmetry codes for the high-temperature phase: (i) $x, y, z + 1$; (ii) $-x, -y + 1, -z + 1$; (iii) $-x + 1, -y + 1, -z + 1$; (iv) $-y + 1, x - y + 1, z + 1$; (v) $y, -x + y, -z + 1$; (vi) $y, -x + y + 1, -z + 1$; (vii) $-x + y, -x + 1, z + 1$; (viii) $x - y, x, -z + 1$; (ix) $x - y + 1, x + 1, -z + 1$; (x) $y, -x + y, -z$; (xi) $-y, x - y, z$; (xii) $-x + y, -x, z$; (xiii) $x - y, x, -z$; (xiv) $-x, -y, -z$; (xv) $-x, -y, -z + 1$; (xvi) $-y + 1, x - y + 1, z$; (xvii) $-x + y, -x + 1, z$; (xviii) $x - 1, y - 1, z$; (xix) $x, y - 1, z$; (xx) $-x, -y + 1, -z + 1$; (xxi) $-x + 1, -y + 1, -z + 1$.

* The values in parentheses are for distances corrected for the thermal movement.

Table 7. *Components of the atomic displacement vectors Δ (in fractional coordinates of the pseudo-hexagonal unit cell) and their absolute values (Å) with e.s.d.'s in parentheses*

Notation of atoms is the same as in Table 3.

Δ	Δx	Δy	Δz	$|\Delta|$
K(1)—K(1)ᴬ	0.0222 (3)	0.0154 (3)	0.00000 (4)	0.116 (1)
K(1)—K(1)ᴮ	0.0068 (3)	0.0222 (3)	0.00000 (4)	0.116 (1)
K(1)ᴬ—K(1)ᴮ	−0.0154 (4)	0.0068 (3)	0.00000 (4)	0.116 (2)
K(2)—K(2)ᴬ	0.0535 (2)	0.0267 (2)	0	0.272 (1)
K(2)—K(2)ᴮ	0.0267 (2)	0.0535 (2)	0	0.272 (1)
K(2)ᴬ—K(2)ᴮ	−0.0268 (2)	0.0268 (2)	0	0.272 (1)
Se—Seᴬ	0.0152 (1)	0.0045 (1)	0.00000 (1)	0.0790 (5)
Se—Seᴮ	0.0106 (1)	0.0151 (1)	0.00000 (1)	0.0790 (5)
Seᴬ—Seᴮ	−0.0045 (1)	0.0106 (1)	0.00000 (1)	0.0790 (5)
O(1)—O(1)ᴬ	−0.0550 (13)	−0.0147 (16)	0.0000 (1)	0.289 (7)
O(1)—O(1)ᴮ	−0.0402 (16)	−0.0549 (13)	0.0000 (1)	0.289 (5)
O(1)ᴬ—O(1)ᴮ	0.0148 (18)	−0.0402 (18)	0.0000 (1)	0.289 (11)
O(2)—O(4)ᴬ	0.0356 (11)	0.0132 (10)	−0.0072 (4)	0.213 (6)
O(2)—O(3)ᴮ	0.0233 (11)	0.0353 (7)	−0.0192 (3)	0.341 (4)
O(3)ᴮ—O(4)ᴬ	0.0123 (10)	−0.0221 (10)	0.0120 (4)	0.253 (6)
O(3)—O(2)ᴬ	0.0353 (7)	0.0121 (10)	0.0192 (3)	0.342 (4)
O(3)—O(4)ᴮ	0.0222 (10)	0.0346 (10)	0.0120 (4)	0.253 (5)
O(2)ᴬ—O(4)ᴮ	−0.0131 (10)	0.0225 (10)	−0.0072 (4)	0.213 (7)
O(4)—O(3)ᴬ	0.0345 (10)	0.0124 (10)	−0.0120 (4)	0.253 (6)
O(4)—O(2)ᴮ	0.0225 (10)	0.0355 (11)	0.0072 (3)	0.213 (5)
O(2)ᴮ—O(3)ᴬ	0.0120 (11)	−0.0231 (11)	−0.0194 (3)	0.341 (5)

Table 8. *Bond-valence sums of corresponding atoms of the low- and high-temperature structures of $K_3Na(SeO_4)_2$, $K_3Na(CrO_4)_2$ and $K_3Na(SO_4)_2$ with e.s.d.'s in parentheses*

	LTP	HTP	$K_3Na(CrO_4)_2$	$K_3Na(SO_4)_2$
K(1)	1.180 (6)	1.119 (6)	1.158 (5)	1.391 (8)
K(2)	0.908 (4)	0.817 (3)	0.906 (4)	1.001 (4)
Na	1.257 (6)	1.200 (6)	1.317 (5)	1.241 (5)
Se	6.122 (29)	6.235 (28)	6.081 (22)	6.036 (29)
O(1)	2.027 (12)	2.041 (20)	2.000 (16)	1.945 (25)
O(2)	2.132 (13)	2.107 (12)	2.117 (92)	2.201 (10)
O(3)	2.108 (12)	—	—	—
O(4)	2.118 (21)	—	—	—
∅[O(2),O(3),O(4)]/O(2)	2.097	2.107 (12)	2.117 (92)	2.201 (10)

to the cation binding in the LTP and HTP as well as in $K_3Na(CrO_4)_2$ and $K_3Na(SO_4)_2$, the bond valences (Brown & Altermatt, 1985) were calculated (Table 8). Bond valences offer a simple comparison of atom binding between similarly coordinated atoms where the respective central and coordinated atoms are of the same species. Because of their exponential dependence on the distances between a central atom and surrounding atoms bond valences are more sensitive than mere averaging of these distances, especially in cases of irregular coordination polyhedra. The values given in Table 8 in addition to the interatomic distances indicate that K(2) is the most loosely bound cation either in the HTP or LTP. This is in accordance with the temperature factor of this cation being the largest and having the largest displacement shift of all the heavy atoms (Table 7).

It should also be noted that the differences in the bond-valence sums between K(1) and K(2) are mainly as a result of the presence of the short K(1)—O(1) bond. The bond-valence sums also suggest that the bonding strength of the K(2) atom increases in the sequence $K_3Na(SeO_4)_2 <$

$K_3Na(CrO_4)_2 < K_3Na(SO_4)_2$. This accounts for the trend of decreasing phase-transition temperatures in this sequence [in $K_3Na(SO_4)_2$ this has not been observed above 100 K]. So, we may conclude that the ferroelastic phase transition in this sequence, which is accompanied by the rotation of tetrahedral anions and simultaneous shift of cations, is affected mainly by the bonding of the K(2) cation. On the other hand it is reasonable to expect that the bonding of the K(2) cation is also a function of the size of tetrahedral anion. The larger anion is expected to cause the atom K(2) to be located in a larger cavity, and therefore be more loosely bound. Thus $K_3Na(MoO_4)_2$ and $K_3Na(WO_4)_2$ at room temperature may also be monoclinic and ferroelastic, though the powder data (PDF 28-801 and PDF 28-802, respectively) do not report doubling of the c axis.

The growing intensity – when the temperature is lowered – of the reflections which develop below the phase transition at 346 K seems to indicate an increasing structural distortion from the parent phase.

Concluding remarks

A precession photograph of $K_3Na(CrO_4)_2$ has revealed that the c axis also doubles its length below the ferroelastic phase-transition point. Thus the low-temperature phases of $K_3Na(SeO_4)_2$ and $K_3Na(CrO_4)_2$ are most probably isostructural. The structure determination of the ferroelastic phase of $K_3Na(CrO_4)_2$ is now being examined.

References

ABRAHAMS, S. C. & KEVE, E. T. (1971). *Ferroelectrics*, **2**, 129–154.
BECKER, P. J. & COPPENS, P. (1974). *Acta Cryst.* A**30**, 129–147.
BERGERHOFF, G., HUNDT, R., SIEVERS, R. & BROWN, I. D. (1983). *J. Chem. Inf. Comput. Sci.* **23**, 66–69.
BROWN, I. D. & ALTERMATT, D. (1985). *Acta Cryst.* B**41**, 192–197.
BUSING, W. R. & LEVY, H. A. (1964). *Acta Cryst.* **17**, 142–146.
CROMER, D. T. & MANN, J. B. (1968). *Acta Cryst.* A**24**, 129–144.
GAULTIER, M. & PANNETIER, G. (1972). *Rev. Chim. Miner.* **9**, 271–289.
HALL, S. R. (1981). *Acta Cryst.* A**37**, 517–525.
KRAJEWSKI, T. (1990). Personal communication.
KRAJEWSKI, T., MROZ, B., PISKUNOWICZ, P. & BRECZEWSKI, T. (1990). *Ferroelectrics*, **106**, 225–230.
KRAJEWSKI, T., PISKUNOWICZ, P. & MROZ, B. (1993). *Phys. Status Solidi A*, **135**, 557–564.
MADARIAGA, G. & BRECZEWSKI, T. (1990). *Acta Cryst.* C**46**, 2019–2021.
MROZ, B., KIEFTE, H., CLOUTER, M. J. & TUSZYNSKI, J. A. (1992). *Phys. Rev. B*, **46**, 8717–8724.
NARDELLI, M. (1983). *Comput. Chem.* **7**, 95–98.
OKADA, K. & OSSAKA, J. (1980). *Acta Cryst.* B**36**, 919–921.
OKADA, K., OSSAKA, J. & IWAI, S. (1979). *Acta Cryst.* B**35**, 2189–2191.
PETŘÍČEK, V. & MALÝ, K. (1988). *The SDS System.* Program package for X-ray structure determination. Institute of Physics, Czechoslovak Academy of Sciences, Praha, Czechoslovakia.
PONTONNIER, L., CAILLET, M. & ALEONARD, S. (1972). *Mater. Res. Bull.* **7**, 799–812.
STEWART, J. M., KRUGER, G. J., AMMON, H. L., DICKINSON, C. W. & HALL, S. R. (1972). The *XRAY* system – version of June 1972. Tech. Rep. TR-192. Computer Science Center, Univ. of Maryland, College Park, Maryland, USA.

Structure of C_{60}: Partial Orientational Order in the Room-Temperature Modification of C_{60}

BY HANS-BEAT BÜRGI

Laboratory of Crystallography, University of Bern, Freiestrasse 3, CH-3012 Bern, Switzerland

AND RENZO RESTORI AND DIETER SCHWARZENBACH

Institute of Crystallography, University of Lausanne, BSP, CH-1015 Lausanne, Switzerland

Abstract

Using published synchrotron X-ray data, the room-temperature scattering density distribution of pure C_{60} has been parametrized in terms of a combination of eight oriented symmetry-related images of the molecule, and of a freely spinning molecule. Corresponding populations are 61 and 39%. The oriented